

Title: **Mean Solar Magnetic Field from Photospheric Vector Magnetograms of Active Regions** (?)

Mean field dynamo theory enables one to explain basic properties of the solar cycle such as 22-year cyclicity and latitudinal migration of the magnetic activity belts with the solar cycle, usually visualised by sunspots of alternate polarity in each 11 year half-cycle. The signs of the magnetic field in each hemisphere are opposite, and change with 22 year magnetic cycle. This is usually formulated as Hale's polarity law and this kind of dynamo model belongs to oscillatory dipole type.

The mechanism of formation of sunspots due to buoyancy instability of magnetic loops has been stipulated since seminal paper by Parker's (1955), see also Parker (1979). Therefore, it is believed that the leading and following spots in each group are linked above the photosphere, and this point of view has numerous observational evidence, from traditional photometric and spectroscopic observations up to visualisation of magnetic arcades and loops in the corona by soft X-ray observations. Sunspot groups, however, often have complex structure and identification of such links between one and the other polarity may become a difficult task. Furthermore, the leading (west-most) sunspots in a group are usually more compact and comprise of structures with stronger magnetic field; therefore, they can be better resolved with available solar magnetograph technique. Therefore, due to limited field of view of magnetograms, there may be substantial imbalance in the average magnetic flux towards the sign of the leading sunspot group.

With progress of numerical simulations there have been developed detailed models of such mechanism of sunspot formation (e.g., Rempel and Schussler, 2000s, see also Rempel et al. 2013-2014).

Recently alternative mechanisms of sunspot formations have been proposed. Using the idea of negative effective magnetic pressure suggested by Kleeorin, Ruzmaikin and Rogachevskii (1980s), Brandenburg et al (2011), also see Kapyla et al. (2012), Kemel et al. (2013 <http://adsabs.harvard.edu/abs/2013SoPh..287..293K>), Warneke et al. (2015 <http://adsabs.harvard.edu/abs/2015arXiv150203799W>) and references therein, have been developed a series of DNS self-contained models describing the instability, and dynamics of magnetic loops, leading to formation of bipolar structures like sunspot groups. According to these calculations, horizontally stretched magnetic flux tubes may either rise or sink depending on the conditions of solar turbulence and the presence of initial (mean) magnetic field. Being numerically and model-parameters robust, such mechanism poses a good alternative compliment to widely adopted Parker's mechanism of sunspot formation.

The information on the observational proxies of the mean magnetic field is extremely important for dynamo theory. Mean values of azimuthal and meridional vector components of magnetic field have been computed in the past (e.g. Ulrich and Boyden, 2005; 2010), and they demonstrate general agreement with Hale's polarity law as well as 22 year cyclic variation along with the main dipolar component of magnetic field of the Sun .

Observations.

In our paper we used systematic vector magnetogram data on solar active regions over the two subsequent cycles 22 and 23 (1988-2005) obtained at Huairou Solar Observing Station, National Astronomical Observatories of Chinese Academy of Sciences.

We used the procedure of de-projection of the magnetograms from the image plane to the tangential to the local solar surface. The procedure of 180 degree disambiguation has been carried out prior to de-projection. For these de-projected data we furthermore computed mean azimuthal B_{ϕ} (East-West),

meridional B_{θ} (North-South) and radial B_r (vertical) components of magnetic field, as well as mean current helicity, averaged the data over the field of view for each active region, and then computed statistical averages over spatially-temporal intervals of 7 degrees latitude and running 2 year time, in much the same way as have been employed by Zhang et al. (2010).

The Interpretation.

Locally at the solar surface, B_{ϕ} has a meaning of the toroidal field, while the field has been transformed during the sunspot formation process, it may hold some properties of the original toroidal field inside the solar convection zone. Magnetic flux tubes in the rotating solar convection zone are subject of Coriolis force that produces tilt of bipolar structures. This mechanism may be responsible for formation of meridional component of magnetic fields, and is parametrised in simple dynamo models by the so-called α -parameter. In very simple terms, arising toroidal field B_{ϕ} produces new-born poloidal flux $B_{\theta} = (C_{\alpha} * B_{\phi})$, where the coefficient C_{α} can be estimated from the magnitude of the α -effect as follows $\alpha * \sqrt{\tau / \eta_T}$ where subscript $*$ denotes typical value, τ the sunspot forming flux tube rising time, and d characteristic depth of sunspot formation. Practically, however, the magnitude of the meridional component of observable field is comparable with azimuthal component.

or
of
diff.

Data Reduction.

In our data analysis, for the 18-year period 1988-2005 covering most of solar cycles 22 and 23, we have used over 6600(?) vector magnetograms taken at various times which represent 983 individual active regions. We have grouped the data into 88 statistically significant sub-groups, binning the data by two-year running intervals by time, and 7 degree intervals in latitude; each of them contains greater than 30 individual magnetograms. Thus, we obtained the values of averaged magnetic field components that we interpret the mean magnetic field. Furthermore we specially focused on those sub-groups for which the means of these values are greater than the 90% Student's confidence interval. The constructed quantities match with Hale's polarity law as well as are in accord with the basic idea of oscillatory dipole type solution to the solar dynamo.

So, we obtained that the Hale's polarity law is pretty well conformed to the observational structure. However, there are a few (10 out of 88) spatially-temporal intervals where there is a statistically significant reversal of the Hale's law.

[

A few hundred of magnetograms in these areas (see the list below) need to be checked for quality (exclude some magnetograms which may have (L,Q,-U)-problem).

]

The reversal of Hale's law occurs near the edges of butterfly wings.

List of time-latitudinal intervals for which the sign of horizontal field components is statistically significant reversed with respect to Hale's law:

Cycle 22:

1. 1988-1989 = N28-N35 = for B_{θ} (*)
2. 1989-1990 = N28-N35 = for B_{ϕ} (*)

3. 1995-1996 = S07-S00 = for B_{ϕ} and B_{θ}
4. 1995-1996 = S14-S04 = for B_{θ}
5. 1996-1997 = S07-S00 = for B_{ϕ} and B_{θ} (*)

Cycle 23

6. 1998-1999 = S14-S07 = for B_{θ} (*)
7. 1999-2000 = S07-S00 = for B_{ϕ}
8. 2002-2003 = N00-N07 = for B_{ϕ} (*)
9. 2002-2003 = S14-S07 = for B_{θ}
10. 2003-2004 = N00-N07 = for B_{ϕ}

B_{ϕ}

(*)=note that the sign B_r is also reversed

Results.

We can interpret the obtained results as follows:

The part of the observed magnetic field in solar active regions that direction is in accord with Hale's polarity law is mostly formed in the photosphere by Parker instability, based on buoyancy of flux tubes. This forms core parts of solar active regions where the flux tube rises above and fall under the photosphere in the leading or following spots. Major sunspot groups of bigger scale active regions are probably due to this mechanism. There always are some other parts of active regions where the magnetic field is directed opposite to the Hale's law. This anti-Hale polarity phenomenon is statistically significant and manifested by the parts of the sunspots that are magnetically linked with the other far-away activities such as other spots, plages and network fields. These parts of the active regions may be formed by another kind of instability, possibly with Negative Effective Magnetic Pressure Instability (NEMPI). Minor sunspot groups at the edges of Butterfly Diagram wings, particularly in higher latitudes or near the equator may well be due to this effect. Furthermore, sunspot groups near the equator may reconnect across the equator where the opposite polarity can leak from one hemisphere to the other. Zhang et al. (2012) (also see refs. therein) have shown that such near-equator active regions are often connected by trans-equatorial loops. Such magnetic loop linkage between the solar hemispheres may cause dynamics in the north-south asymmetry (see Pipin et al. 2014 and references therein), and also be an agent for interaction of solar dynamo waves in both hemispheres, capable for causing global modulation of the solar sunspot cycle on secular time scales, such as Gleissberg cycle (see e.g. Galitski et al., 2005).

Another by-product of this computation is that the general solar-cycle pattern for the current helicity as obtained earlier by Zhang et al. (2010) holds as the magnetograms are de-projected from the image plane to the tangential to the solar surface, although the mixture of high accuracy longitudinal and less sensitive transverse components of the observable magnetic field after correction for projection effects may increase the error in computation of helicity parameters.

In our Discussion, we may impute the phenomenon of reversal of Hale's law to

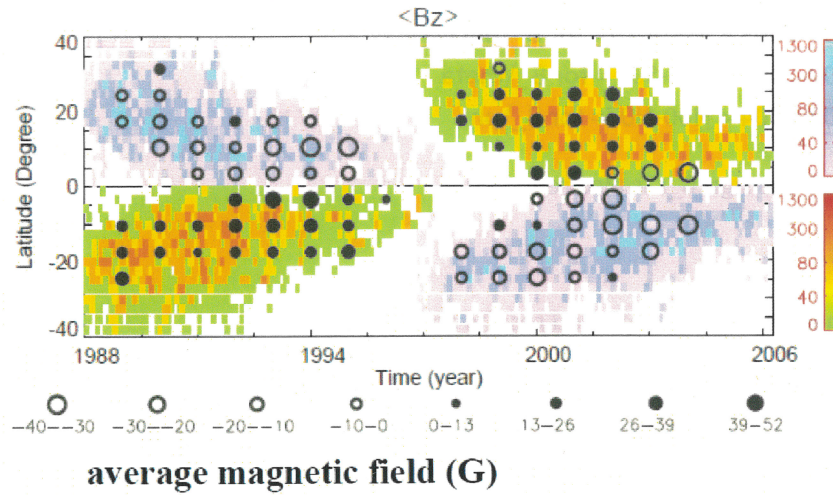
- (a) Mechanism of sunspot formation, alternative to Parker's
- (b) Phase shift in evolution of the toroidal and poloidal components of the mean magnetic field

This discussion can be further developed later.

Figures:

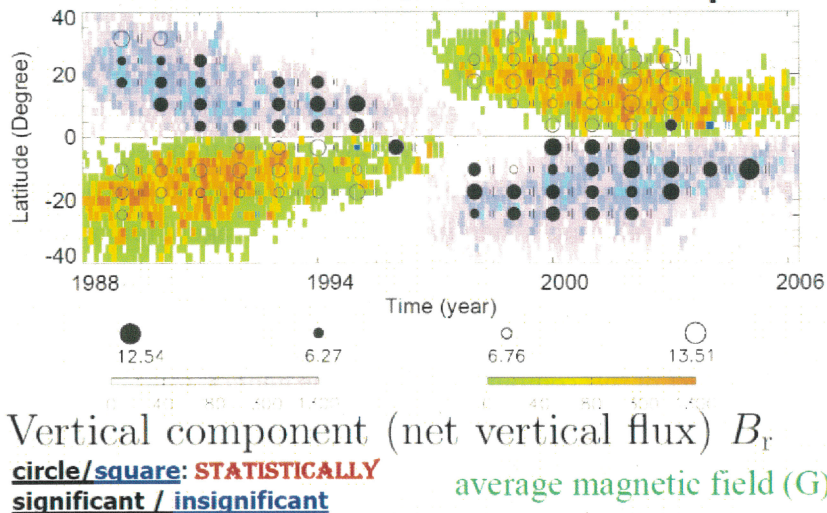
- 1) Original Longitudinal field averaged $\langle B_z \rangle$ before de-projection correction for projection effects

The Longitudinal Magnetic Field: Hale's Polarity Law for $\langle B_z \rangle$



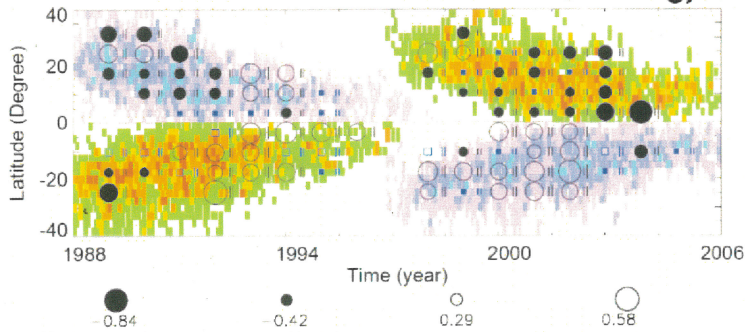
- 2) De-projected vertical component $\langle B_r \rangle$ (net flux)

The vertical net magnetic flux: Hale's Polarity Law for $\langle B_r \rangle$



6) Current helicity for de-projected results.

Hemispheric rule for vertical part of electric Current Helicity $\langle H_{cr} \rangle$



Current helicity H_{cr} overlaid with sunspot density)
average helicity density ($10^{-3}G^2/m$)

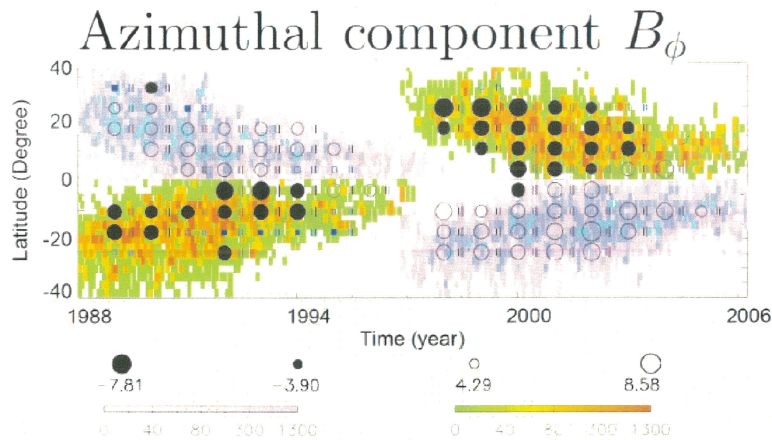
circles/squares: **STATISTICALLY significant / insignificant**

----- Table: total 87 bin =100% from analysis of Figures 2- 4, 6 and comparison with Zhang et al. (2010)

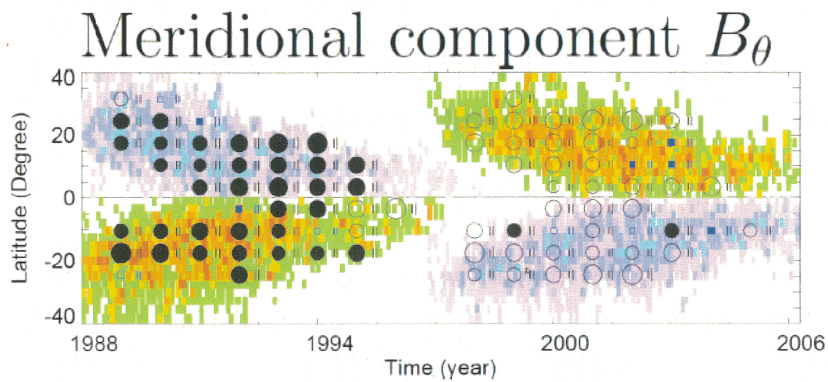
Quantity	B_r	B_phi	B_theta	H_cr		H_cz(2010)	
Reversed Significantly	5 (6%)	6 (7%)	6 (7%)	13	15%	18/87 =21%	18/88 =20%
Reverse Insignificantly	3	7	7	5	22/87 =25%		
Accord Insignificantly	2	4	4	17		69/87 =79%	70/88 =80%
Accord Significantly	77 (89%)	70 (80%)	70 (80%)	52 (80%)	60%		

7) Illustrations of vector magnetograms which obey and disobey Hale's law.

- 3) De-projected azimuthal component $\langle B_{\phi} \rangle$

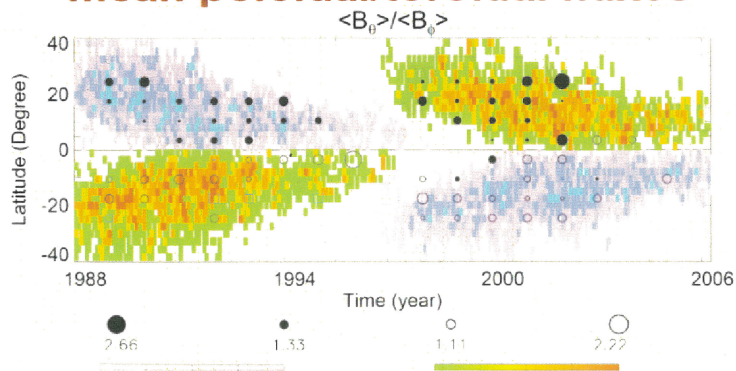


- 4) De-projected meridional component $\langle B_{\theta} \rangle$



- 5) Ratio of $\langle B_{\theta} \rangle / \langle B_{\phi} \rangle$ as a measure of new-born toroidal field

Hemispheric rule for Ratio of mean poloidal/toroidal fluxes

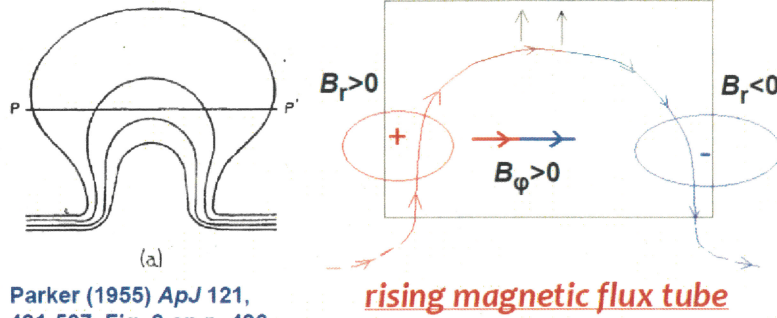


proxy of new-born poloidal field
circles/squares: STATISTICALLY significant / insignificant

- 8) Schematic diagram of the magnetic field in a Sunspot group formed by Parker's mechanism

Parker (1955) mechanism of buoyancy sunspot formation

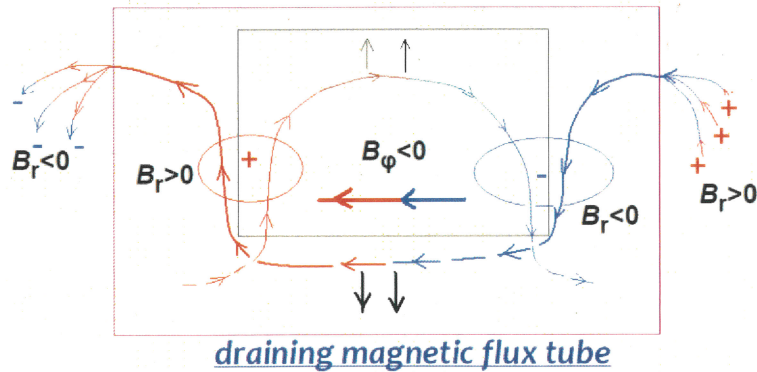
LIMITED FIELD OF VIEW



- 9) Schematic diagram of the magnetic field in a Sunspot group formed by an alternative/complimentary mechanism

non-Parker mechanism of sunspot formation (probably NEMPI)

GREATER FIELD OF VIEW



$$A_p \sim \cancel{st} \cdot \alpha \cdot B_p$$

$$B_\theta \sim \frac{A_p}{d} = \frac{\alpha \cdot st}{d} B_p$$

$$\alpha \sim \frac{1}{R} \quad \alpha = \frac{\alpha \cdot R}{R} \approx 1 \approx \frac{\alpha \cdot 10^{10} \text{ cm}}{10^{12} \frac{\text{cm}^2}{\text{s}} \text{ a few}} \Rightarrow \alpha \sim 10^{\frac{2 \text{ cm}}{\text{s}}} \sim 1 \text{ s}$$

$$st \sim \text{a few days} \approx 24 \cdot 3600 \approx 9 \cdot 10^4 \approx 10^5$$

$$\frac{\text{a few}}{1-10 \cdot 10^6 \text{ m}}$$

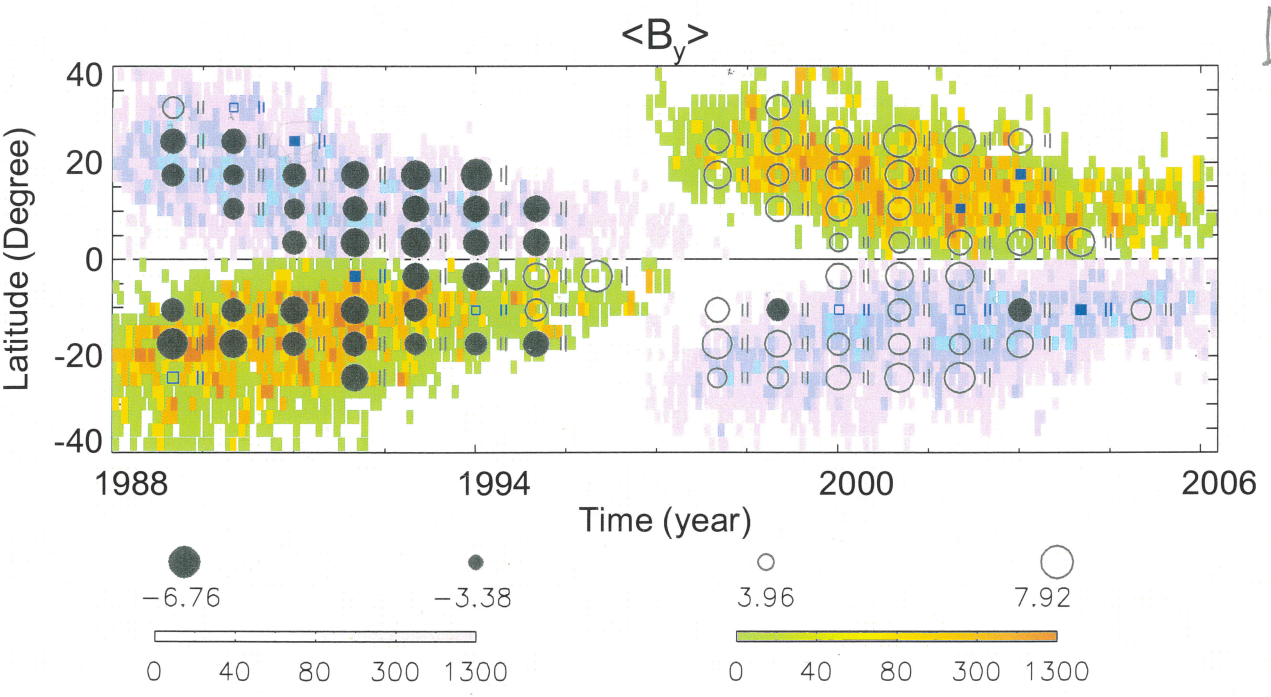
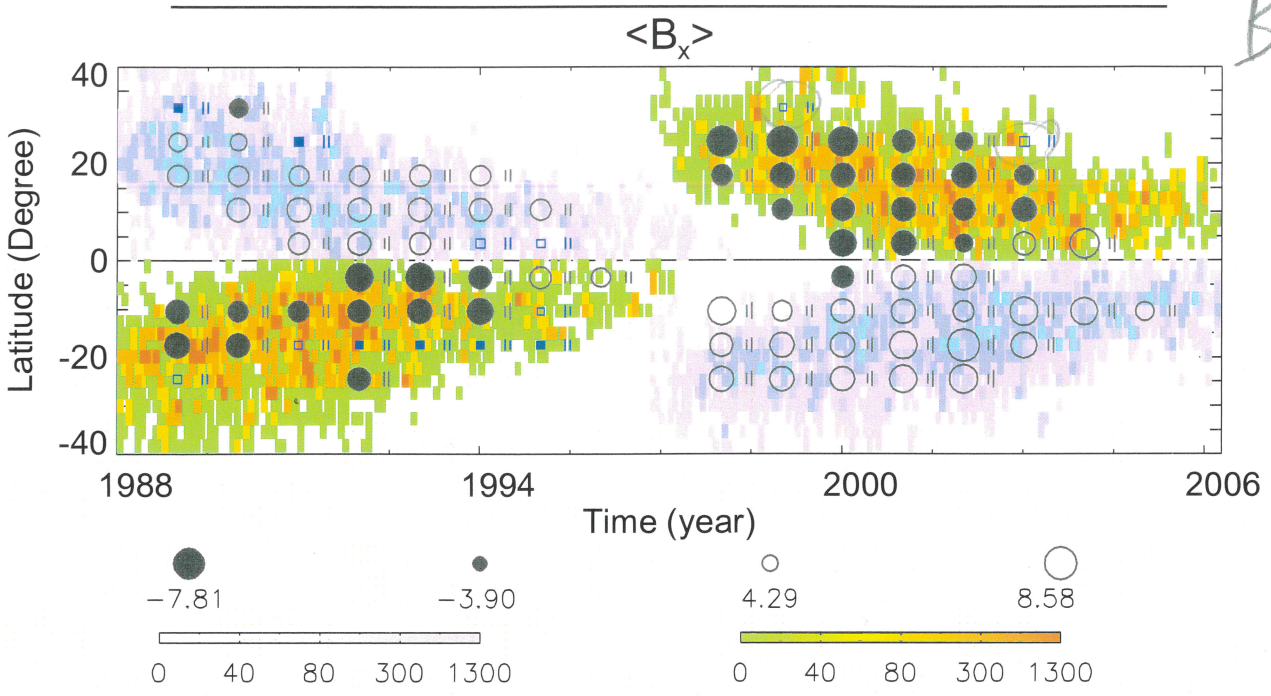
$$\frac{\text{dept} \sim 10 \text{ Mm}}{\text{a few}} \approx \frac{10^7 \text{ m}}{10^7 \text{ m}} \approx 1$$

$$\underline{B_\theta \approx 0.1 B_p}$$

Conf I_{90%} / data

1

B_φ



B_θ

Fig. 1: Azimuthal component B_ϕ . Meridional component B_θ .

$$H_c = \langle B_r \cdot J_r \rangle$$

2

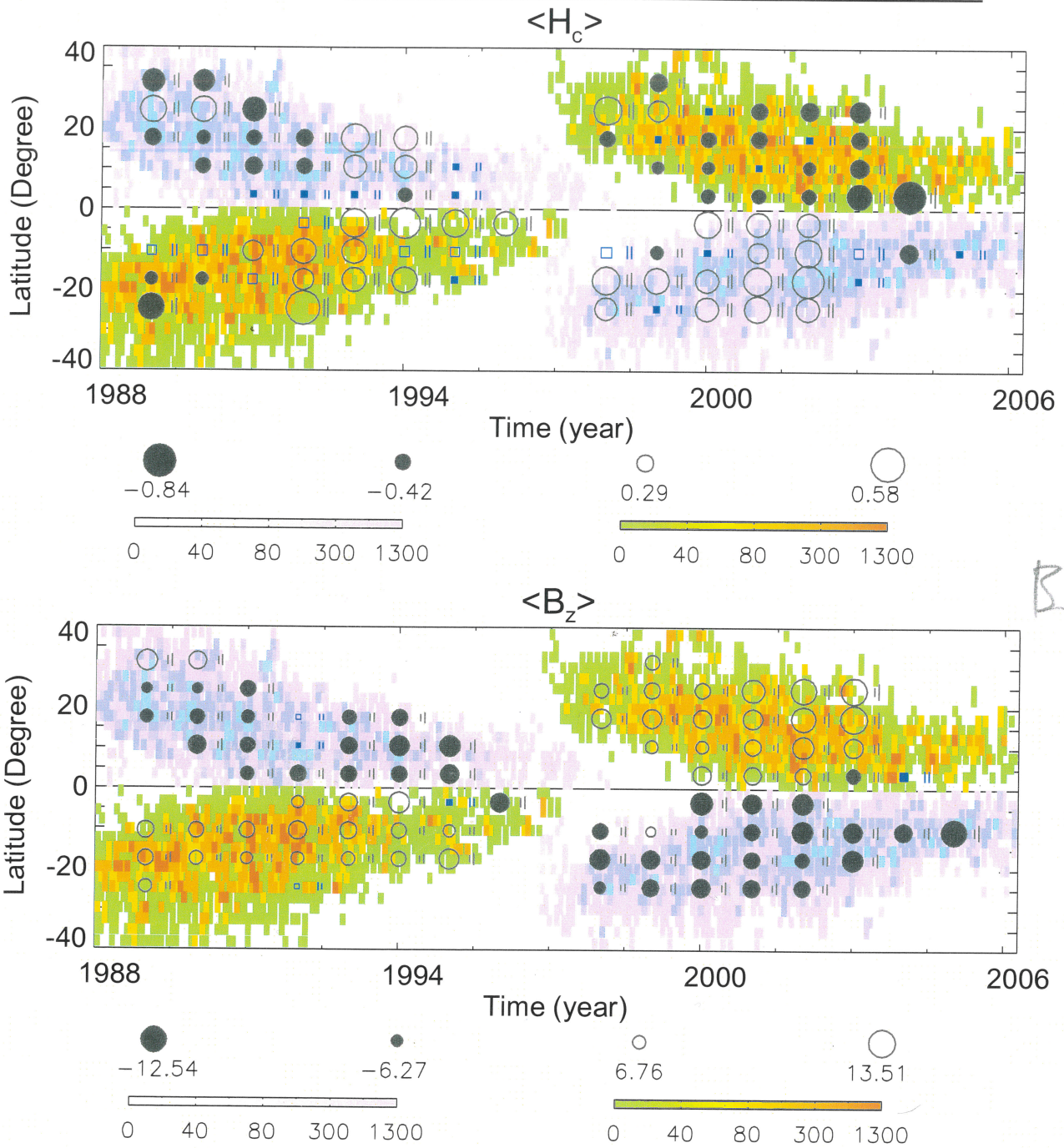
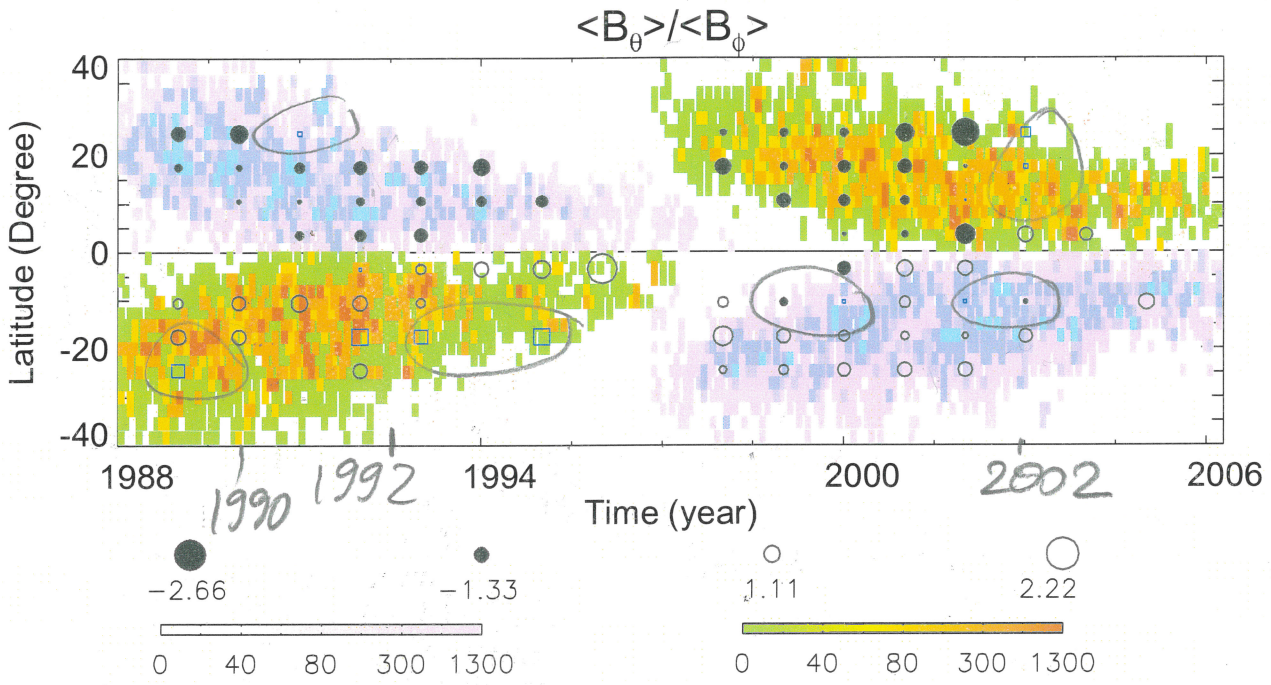


Fig. 2: Current helicity H_{cr} . Vertical component (net vertical flux) B_r .



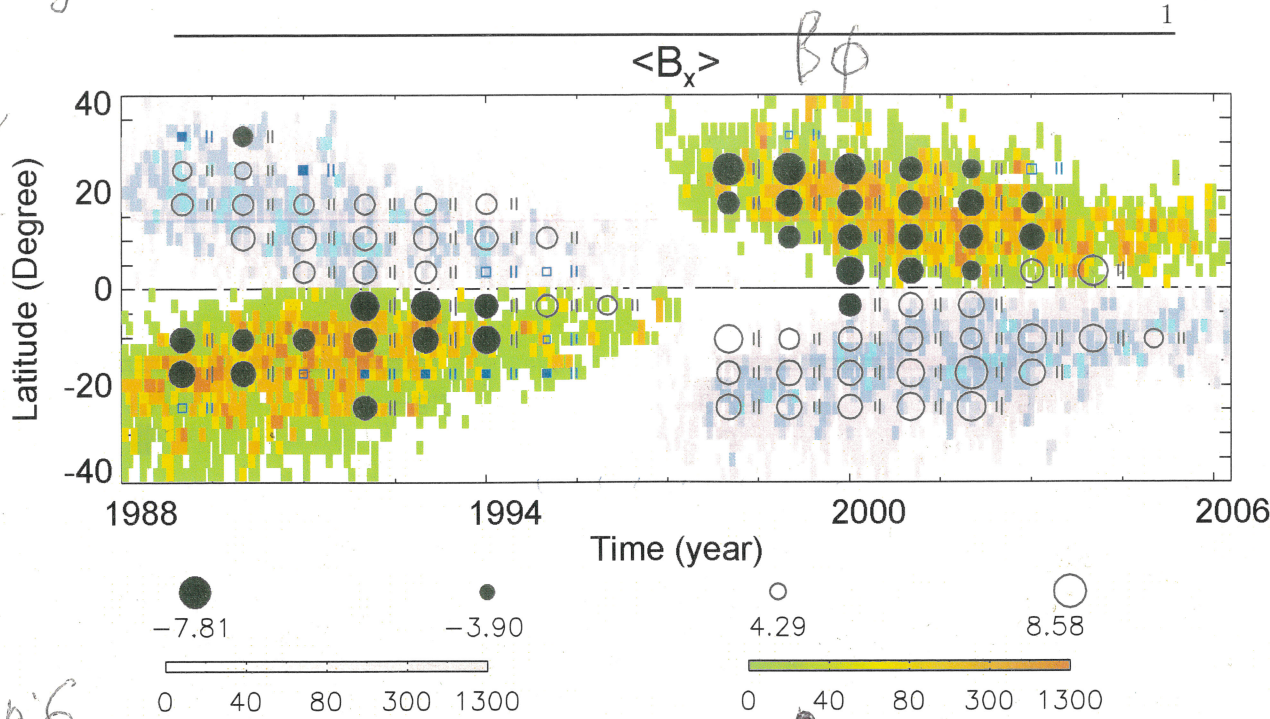
↑
cf. tilt

Fig. 3: Ratio of mean poloidal/toroidal fluxes $\langle B_\theta \rangle / \langle B_\phi \rangle$ (proxy of new-born poloidal field)

$|B_z| > 20$
 $|B_+| > 150$

sign. Rev: 6
insig. Rev: 7
insig obey: 4
obey:
70/87

de-Projected.



Rev. Sign: 6
Rev. insig: 7
obey insig:
obey 70/87

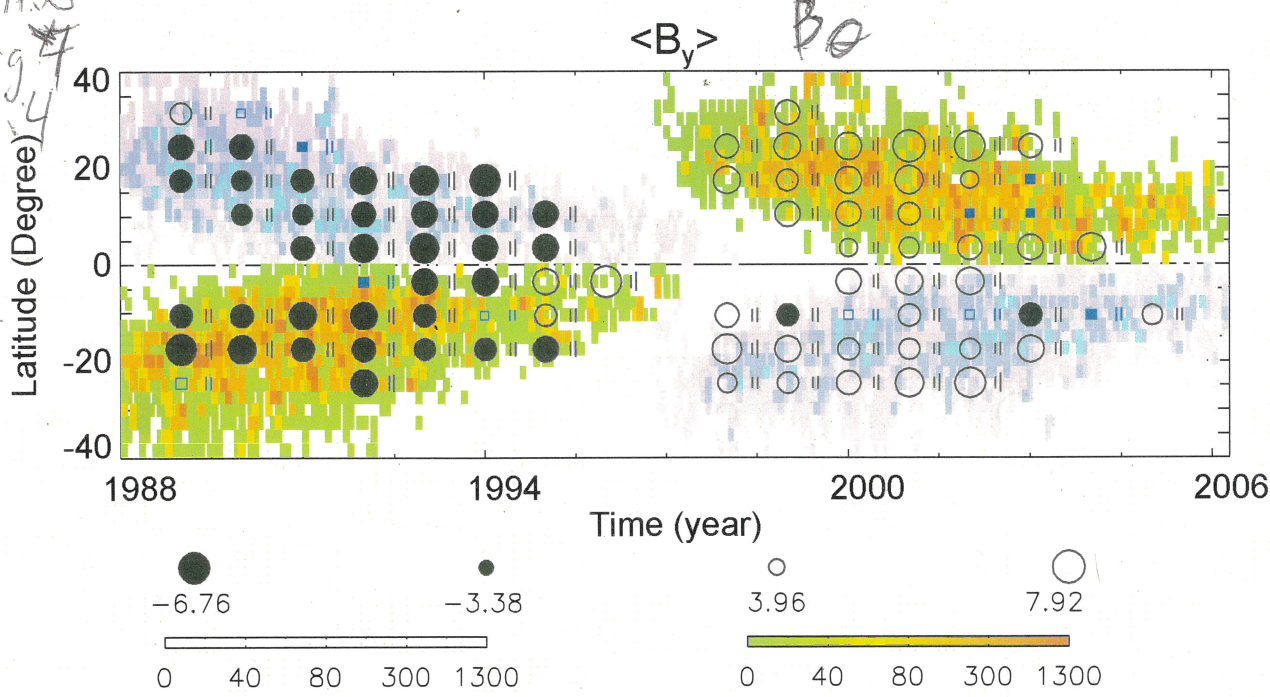


Fig. 1: Azimuthal component B_ϕ . Meridional component B_θ .

Total: 87

revers. sign. disobey: 13(8N+5S)

revers. in sign: 5(south)

deprojected

obey: 52
52/87

sign. Rev. 5
in sign. Rev. 3
in sign. obey: 2
obey: 77
77/87

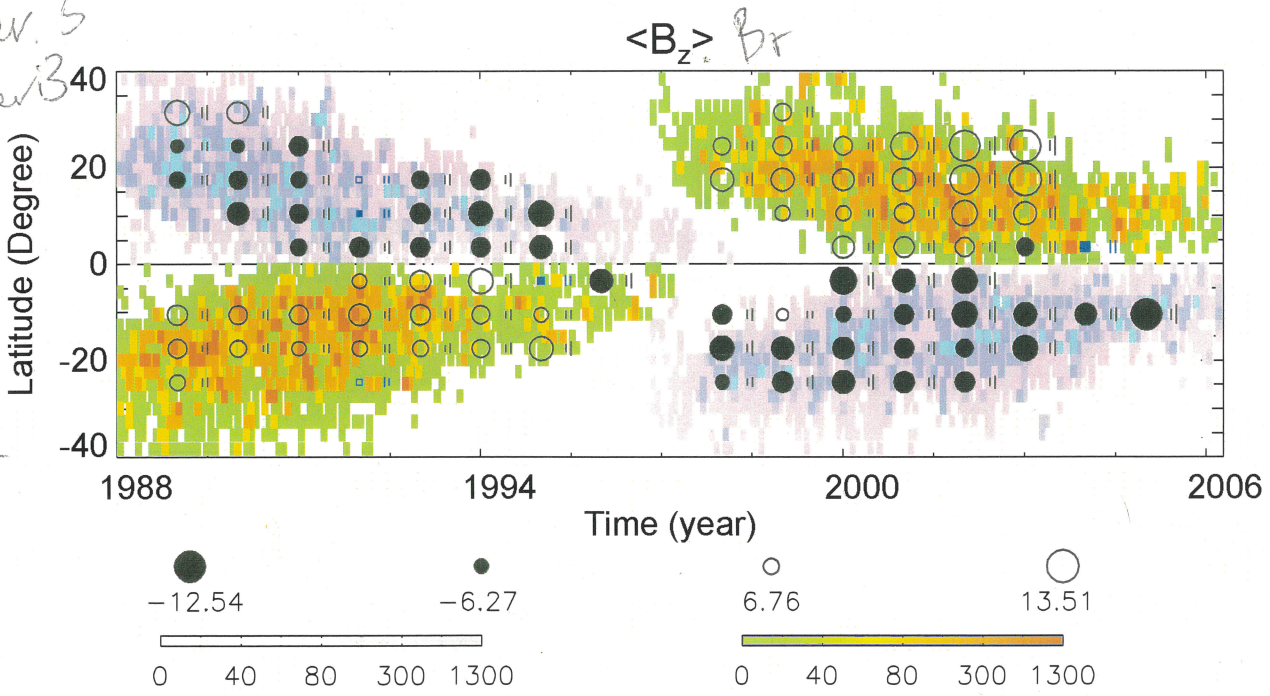
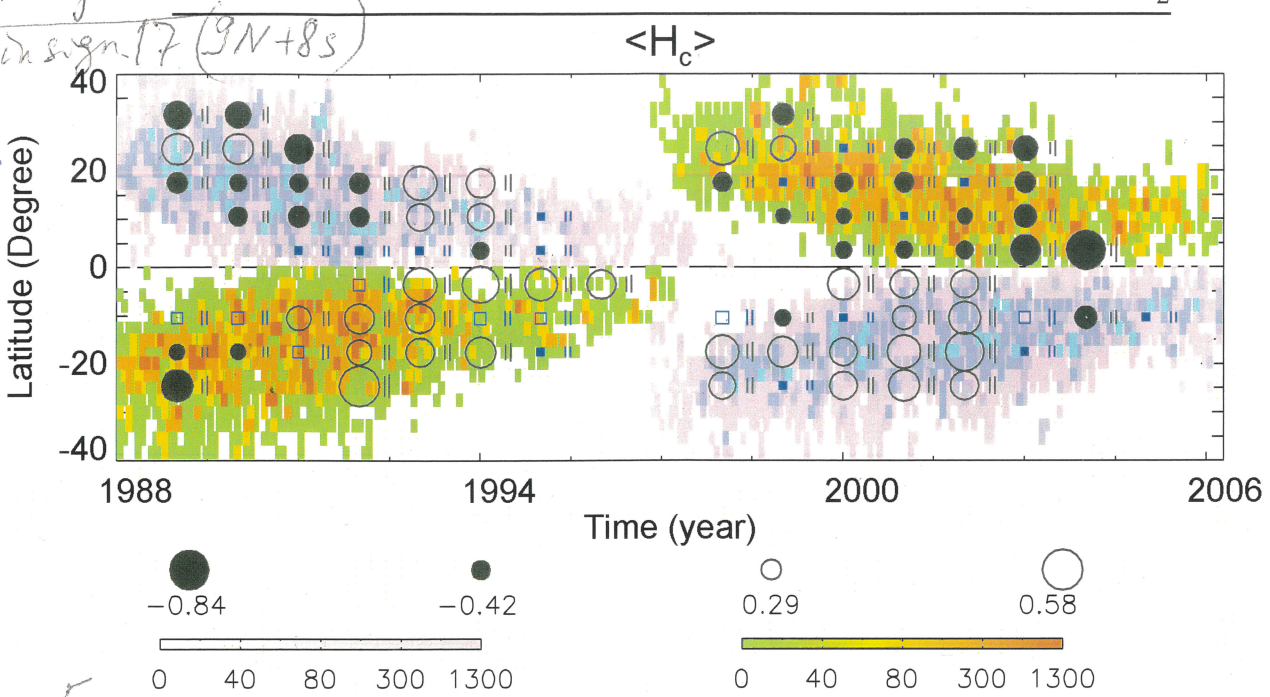
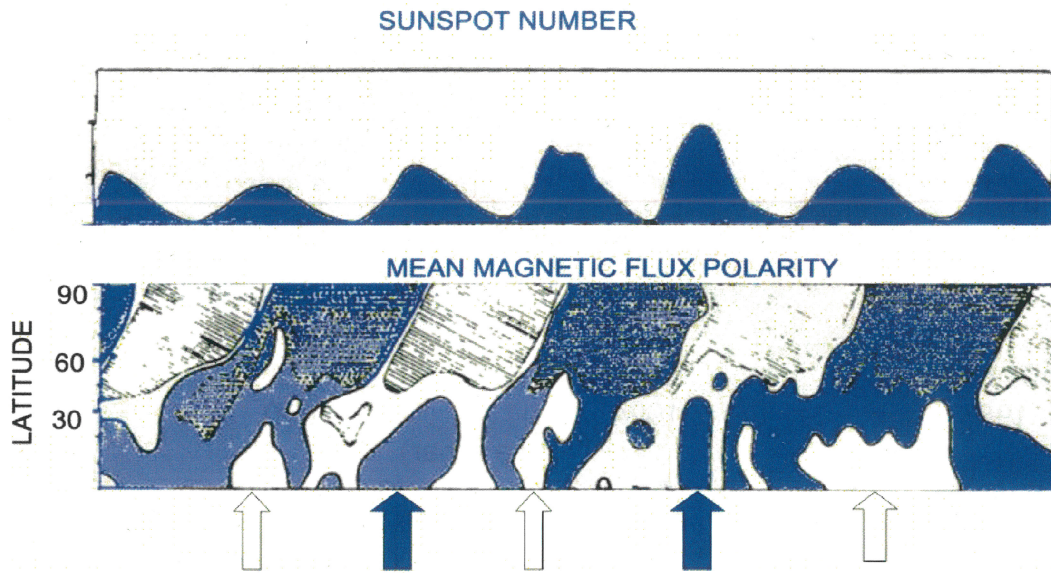


Fig. 2: Current helicity H_{cz} . Vertical component (net vertical flux) B_r .

Obridko & Gaziev (1992)



The location of the precursor is marked with an arrow in the Figure.

Statistical significance
(90% confidence intervals)

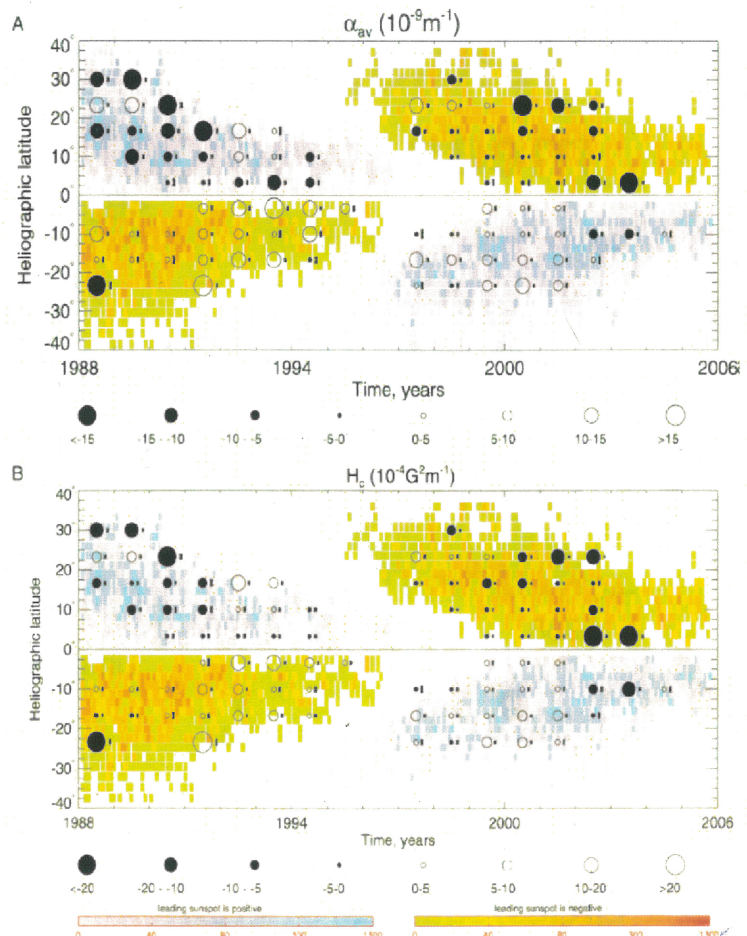
Signal exceeds the error bar level:

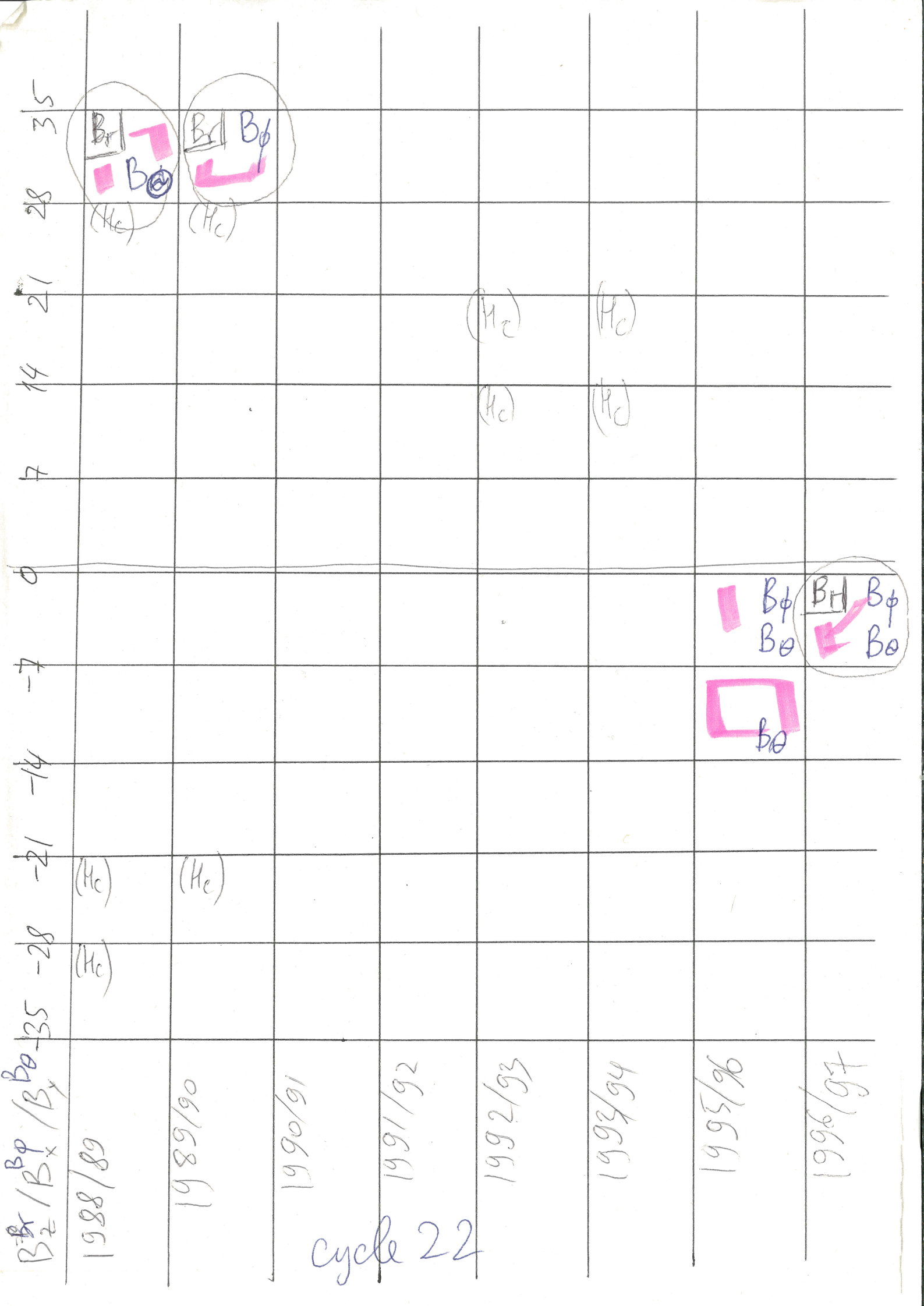
- out of 88 groups:

for H_c : 72 (82%)

for α_{av} : 67 (74%)

(Zhang et al., 2010)





$B_2^x / B_1^p / B_0^p$

1988/89

1989/90

1990/91

1991/92

1992/93

1993/94

1995/96

1996/97

cycle 22

35

28

21

14

7

0

-7

-14

-21

-28

-35

(He)

(He)

(He)

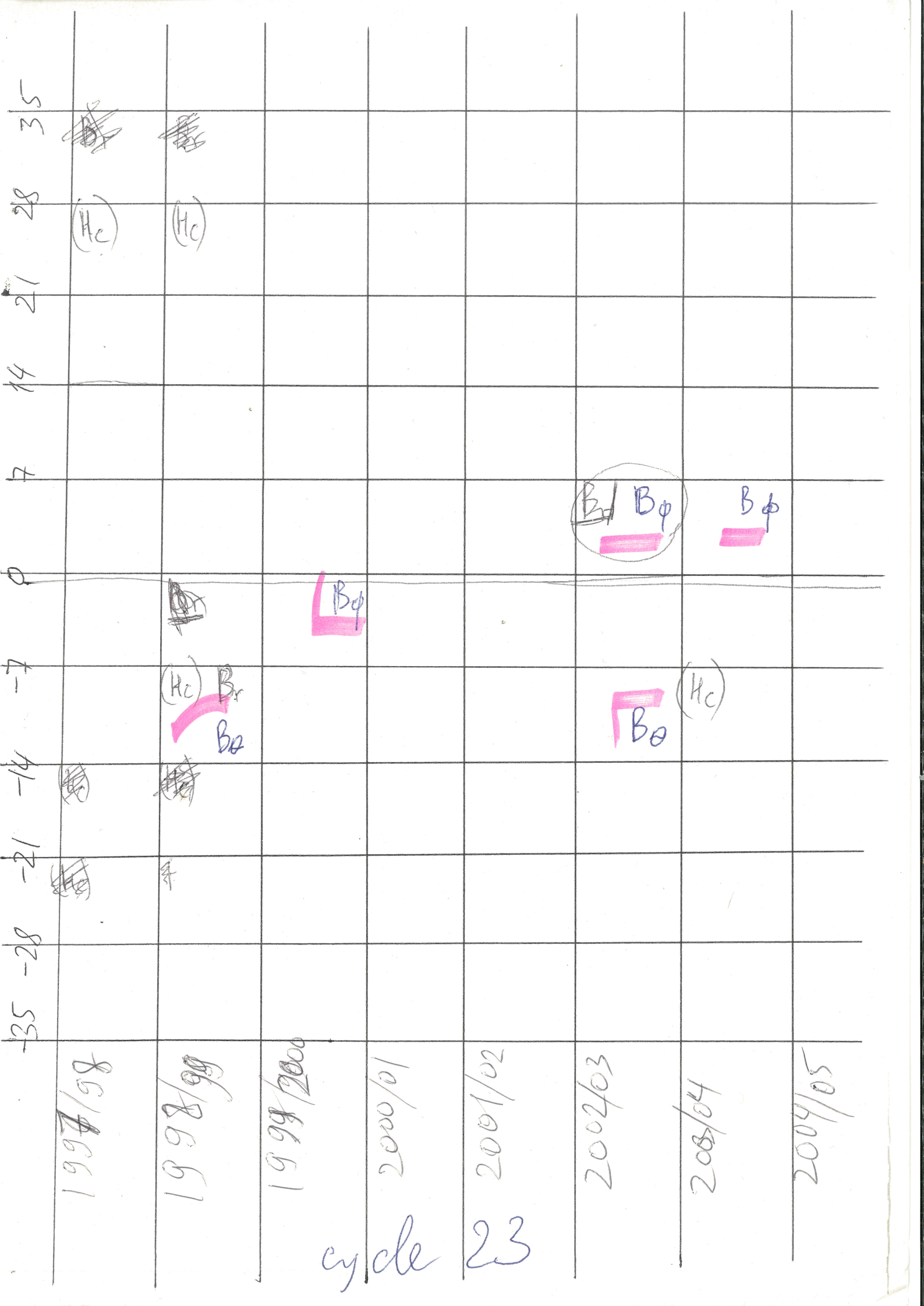
(He)

(He)

(He)

(He)

B_1^p B_0^p B_1^p B_0^p
 B_0^p B_0^p



86/8661
1997/98

86/8661
1998/99

86/8661
1999/2000

cycle 23

2000/01

2001/02

2002/03

2003/04

2004/05